Research Square

Preprints are preliminary reports that have not undergone peer review.
They should not be considered conclusive, used to inform clinical practice,
or referenced by the media as validated information.

Pathogen detection profiles and Mycoplasma pneumoniae macrolide-resistance- associated mutations in pediatric respiratory specimens in Zhuzhou, China: a retrospective multicenter study

Mingkai Yang
Zhuzhou Central Hospital
Zhou Chu
Zhuzhou Central Hospital
Minliang Yan
Zhuzhou Central Hospital
Lian Huang
Xiangdong Hospital Affiliated with Hunan Normal University
Zhaoxia Li
Women And Children Healthcare Hospital Of Zhuzhou
Xirong Fu
Youxian People's Hospital
Yanqin Liu
Chaling County People's Hospital
Yan Chen
Zhuzhou Lukou District People's Hospital
Jinyan Huang
Zhuzhou Second Hospital
Kenheng Zhou
Zhuzhoushi 331 Hospital
Guohong Hu
290171219@qq.com

Zhuzhou Central Hospital

Research Article

Keywords: Children, Respiratory infections, Targeted next-generation sequencing, Pathogen detection profile, Mycoplasma pneumoniae, Macrolide resistance

Posted Date: November 13th, 2026

DOI: https://doi.org/10.21203/rs.3.rs-11223102/v1

License: This work is licensed under a Creative Commons Attribution 4.0 International License.
Read Full License

Additional Declarations: No competing interests reported.

Pathogen detection profiles and *Mycoplasma pneumoniae* macrolide-resistance-associated mutations in pediatric respiratory specimens in Zhuzhou, China: a retrospective multicenter study

Authors: Mingkai Yang[1, 2]; Zhou Chu[1]; Minliang Yan[1]; Lian Huang[3]; Zhaoxia Li[4]; Xirong Fu[5]; Yanqin Liu[6]; Yan Chen[7]; Jinyan Huang[8]; Kenheng Zhou[9]; Guohong Hu[1, 2, *]

Affiliations: 1. Department of Pediatrics, Zhuzhou Central Hospital, Zhuzhou, Hunan, China
2. Department of Pediatrics, Zhuzhou Clinical College, Jishou University, Zhuzhou, Hunan, China
3. Department of Pediatrics, Xiangdong Hospital Affiliated with Hunan Normal University, Zhuzhou, Hunan, China
4. Department of Pediatrics, Women And Children Healthcare Hospital Of Zhuzhou, Zhuzhou, Hunan, China
5. Department of Pediatrics, Youxian People's Hospital, Hunan, China
6. Department of Pediatrics, Chaling County People's Hospital, Zhuzhou, Hunan, China
7. Department of Pediatrics, Zhuzhou Lukou District People's Hospital, Zhuzhou, Hunan, China
8. Department of Pediatrics, Zhuzhou Second Hospital, Zhuzhou, Hunan, China
9. Department of Pediatrics, Zhuzhoushi 331 Hospital, Zhuzhou, Hunan, China

Correspondence: 290171219@qq.com

Abstract

Background: Regional respiratory pathogen surveillance may inform pediatric diagnostic practice. We investigated pathogen detection profiles, age and seasonal distributions, multiple-pathogen co-detection, and *Mycoplasma pneumoniae* macrolide-resistance-associated mutations in Zhuzhou, China.

Methods: We retrospectively analyzed 13,273 respiratory specimens and targeted next-generation sequencing (tNGS) results from children attending eight healthcare institutions in Zhuzhou, China, between January 2023 and December 2025. Pathogen detection profiles, age and seasonal distributions, multiple-pathogen co-detection patterns, and 23S rRNA macrolide-resistance-associated mutations in *M. pneumoniae* were evaluated. Group comparisons used the χ^2 test or Fisher's exact test, with Bonferroni correction for pairwise comparisons.

Results: Pathogens were detected in 12,901 of 13,273 specimens (97.20%), with 32,525 detections of 35 pathogens. The five most frequently detected pathogens were Haemophilus influenzae (40.68%), rhinovirus (30.31%), Streptococcus pneumoniae (25.93%), Moraxella catarrhalis (22.39%), and M. pneumoniae (22.08%). Detection profiles varied by age and season. M. pneumoniae detection was high during July 2023–August 2024 and low in 2025. Multiple pathogens were detected in 77.38% of positive specimens; 94.18% of these had a single pathogen with relative abundance ≥ 50%. Co-detection rates did not differ by specimen type ($P = 0.892$) but varied by age ($P < 0.001$). In the primary analysis, macrolide-resistance-associated mutations were identified in

2,324/2,865 M. pneumoniae-positive specimens (81.12%). This denominator excluded 66 uninterpretable specimens but included 420 without reported resistance results, which were classified as mutation-negative. A2063G accounted for 99.40% of mutation-positive specimens.
Conclusions: Pediatric respiratory specimens in Zhuzhou showed frequent pathogen co-detection and age- and season-specific detection profiles. *M. pneumoniae* macrolide-resistance-associated mutations were common, although missing resistance results affect interpretation. These findings may inform regional surveillance; pathogen detection and read abundance require interpretation alongside clinical evidence.

Keywords: Children; Respiratory infections; Targeted next-generation sequencing; Pathogen detection profile; *Mycoplasma pneumoniae*; Macrolide resistance

Background

Respiratory infections (RIs) are major causes of morbidity, hospitalization, and death in children younger than 5 years. Lower respiratory infections rank second among contributors to the global disease burden in children aged 0–9 years, and pneumonia remains a major threat to child survival(1) [1, 2]. Respiratory infections have diverse etiologies, and two or more pathogens may be detected during a single illness episode. Multiple-pathogen co-detection has been associated with more complex clinical presentations and a greater disease burden [3]. Timely and accurate pathogen identification is therefore important for early targeted management and rational antimicrobial use.

Conventional diagnostic methods, including culture, antigen detection, serology, and single-target nucleic acid tests, can be time-consuming, have limited sensitivity, or cover only a restricted number of pathogens, and may not meet the need for rapid, broad-spectrum etiological diagnosis [4]. Targeted next-generation sequencing (tNGS) enriches target pathogen nucleic acids through primer amplification or hybrid capture and can identify tens to hundreds of pathogens, as well as virulence and antimicrobial-resistance genes [5]. As costs have decreased and workflows have matured, tNGS has been used increasingly for etiological diagnosis of pediatric respiratory infections.

Respiratory pathogen composition and circulation patterns vary substantially by geographic setting. Characterizing local pathogen epidemiology may help reduce biases in empirical treatment and support regional precision medicine [6]. Following adjustment of coronavirus disease 2019 (COVID-19) control measures in China in late 2022, several respiratory pathogens resurged. In particular, *M. pneumoniae* circulated widely during 2023–2024, and pediatric respiratory pathogen profiles changed substantially from the pre-pandemic period [7, 8]. Zhuzhou is located in eastern Hunan Province and within the Changsha–Zhuzhou–Xiangtan urban agglomeration. A large-sample study may therefore improve understanding of the local pathogen profile.

Using tNGS results from children with respiratory infections at eight healthcare institutions in Zhuzhou, we analyzed pathogen detection profiles, age and seasonal distributions, multiple-pathogen co-detection patterns, and macrolide-resistance-associated mutations in *M. pneumoniae*.

Methods

Study design and participants

This retrospective multicenter study included children aged 28 days to 14 years who attended eight healthcare institutions in Zhuzhou, China, between January 2023 and December 2025 and underwent tNGS for respiratory pathogens.

Eligible participants had respiratory-infection-related clinical manifestations and met at least one of the following criteria: (1) fever, cough, rhinorrhea, sore throat, or tachypnea; (2) an abnormal total white blood cell count and/or neutrophil proportion; or (3) inflammatory infiltrates on chest imaging and/or moist rales on pulmonary auscultation. Participants were also required to have a respiratory specimen tested by tNGS and complete information on age, sex, specimen type, and test results. Children with congenital immunodeficiency, airway malformations, non-respiratory infections, or non-infectious respiratory diseases were excluded, as were those lacking age or other key demographic data. The primary unit of analysis was the respiratory specimen and its corresponding tNGS result. For children who underwent repeat testing, findings represent pathogen detections at the testing-event level.

Of 13,278 initially available specimens, five were excluded because of missing age information or failure to meet the inclusion criteria. The final analysis included 13,273 respiratory specimens from children.

Specimen collection

Respiratory specimens were collected by trained healthcare professionals within 24 h of the outpatient visit or hospital admission. The 13,273 specimens comprised 12,403 nasal or throat swabs, 47 sputum specimens, and 823 lower respiratory tract lavage specimens, including 795 bronchoalveolar lavage fluid specimens and 28 other lavage specimens. All specimens were stored, transported, and tested by tNGS using a standardized workflow.

tNGS workflow

Samples were liquefied by adding an equal volume of 80 mmol/L dithiothreitol and homogenized. A 500 μL aliquot of the homogenate was used for total nucleic acid extraction and purification with the MagPure Pathogen DNA/RNA Kit (R6672-01B, Magen, Guangzhou, China) according to the manufacturer's protocol.

Libraries were prepared with the Respiratory Pathogen Detection Kit (KS608-100HXD96, KingCreate, Guangzhou, China). Positive and negative controls supplied with the kit and a no-template control were included to monitor the tNGS workflow. Two rounds of ultra-multiplex polymerase chain reaction (PCR) were performed to enrich targeted sequences from bacteria, including *Mycoplasma* and *Chlamydia*, viruses, and fungi. Nucleic acids and reverse-transcribed cDNA were used as templates for target enrichment with 153 microorganism-specific primers. PCR products were purified with magnetic beads and subsequently amplified with sequencing-adapter and barcode-bearing primers. Library quality and quantity were assessed using the Qsep100 Bio-Fragment Analyzer (Bioptic, Taiwan, China) and Qubit 4.0 fluorometer (Thermo Scientific, Massachusetts, USA), respectively. Library fragments were generally 250–350 bp, with a minimum library concentration of 0.5 ng/μL. The pooled library was re-quantified, diluted to 1 nmol/L, denatured with freshly prepared 0.1 mol/L NaOH, and sequenced on an Illumina MiniSeq platform with the universal sequencing reagent kit (KS107-CXR, KingCreate, Guangzhou, China). Each library yielded approximately 0.1 million single-

end reads of 100 bp.

Sequencing data were analyzed with the data management and analysis system (version 3.7.2, KingCreate). Adapter sequences were removed. Reads longer than 50 bp and with a Q30 proportion greater than 75% were retained. Single-end reads were aligned against an in-house clinical pathogen database curated from GenBank, RefSeq, and the NCBI Nucleotide database to quantify reads for each specific amplicon target.

Pathogen positivity was interpreted with reference to the expert consensus on tNGS application in infectious diseases [9], the 2025 expert consensus on etiological diagnosis and clinical management of acute respiratory tract infections in children [10], and guidance for clinical interpretation of bronchoalveolar lavage fluid metagenomic next-generation sequencing results in severe community-acquired pneumonia [11]. Considering specimen type, pathogenicity category, amplicon coverage, and normalized read counts, we applied the following four-tier interpretation rules (Table 1): any detection of a special pathogen was considered positive; established pathogens required at least three specific reads; conditionally pathogenic organisms required a relative abundance greater than 70%; and background organisms and contaminants were not considered positive. Results were reviewed by two trained professionals. The pathogen detection rate was the principal outcome measure.

Table 1. Tiered rules for interpretation of pathogen positivity

Interpretation category	Threshold	Pathogens
Special pathogens	Any detection considered positive	*Mycoplasma pneumoniae*, *Chlamydia pneumoniae*, *Mycobacterium tuberculosis* complex, *Bordetella pertussis*, *Legionella pneumophila*, *Pneumocystis jirovecii*, *Aspergillus fumigatus*, etc.
Established pathogens	≥3 specific reads	*Haemophilus influenzae*, *Streptococcus pneumoniae*, *Moraxella catarrhalis*, *Staphylococcus aureus*, Rhinovirus, Human respiratory syncytial virus, Human adenovirus, Human metapneumovirus, Human parainfluenza viruses types 1–4, Enterovirus, Human bocavirus, Influenza A and B viruses, SARS-CoV-2, Human coronaviruses, Coxsackieviruses, *Chlamydia trachomatis*, etc.
Conditionally pathogenic organisms	Relative abundance >70%	*Streptococcus pyogenes*, *Streptococcus anginosus* group (including *S. anginosus*, *S. intermedius*, and *S. constellatus*), *Acinetobacter baumannii*, *Klebsiella pneumoniae*, *Pseudomonas aeruginosa*, *Bordetella parapertussis*, Human parvovirus, WU polyomavirus, etc.
Background organisms and contaminants	Not considered positive	*Neisseria* spp. and other common upper respiratory tract colonizers; *Staphylococcus* spp., *Prevotella* spp., *Veillonella* spp., *Fusobacterium* spp., and *Candida* spp. as respiratory tract colonizers; and common reagent and environmental background microorganisms

Note: Interpretation was guided by references [9–11]. Relative abundance was defined as the number of reads assigned to a pathogen divided by the total microbial reads in the same pathogen class (bacteria, viruses, or fungi).

Interpretation of macrolide-resistance-associated mutations

For specimens positive for *M. pneumoniae*, 23S rRNA macrolide-resistance-associated mutations were interpreted with reference to the expert consensus on macrolide-resistant *M. pneumoniae* pneumonia in children [12]. Mutant allele frequency (f) was classified as a

predominant mutant population (f ≥ 95%), a mixed population (20% ≤ f < 95%), or no resistance-associated mutation detected (f < 20%). Specimens without a reported resistance-testing result were classified as having no resistance-associated mutation in the primary analysis. Analyses of resistance-associated mutations included only *M. pneumoniae*-positive specimens.

Statistical analysis

Data cleaning, interpretation, statistical analysis, and figure generation were performed using Python and GraphPad Prism. Categorical variables are presented as n (%). Positivity, pathogen detection, multiple-pathogen co-detection, and monthly detection rates were calculated as the number of positive specimens divided by total specimens, the number of specimens positive for a given pathogen divided by the total number of specimens in that group, the number of positive specimens with two or more detected pathogens divided by all positive specimens in that group, and the number of specimens positive for a given pathogen divided by specimens submitted in that month, respectively. Groups were compared with the χ^2 test or Fisher's exact test. Yates' continuity correction was used for 2 × 2 tables. Fisher's exact test was used when more than 20% of cells had expected counts < 5 or any cell had an expected count < 1; Fisher–Freeman–Halton exact testing was used to confirm r × c comparisons. For pairwise comparisons, unadjusted P values were compared with the Bonferroni-corrected significance threshold ($\alpha' = 0.05$/number of comparisons). In specimens with multiple pathogens, relative abundance was calculated from the proportion of reads assigned to each pathogen; a pathogen with a relative abundance ≥ 50% was considered dominant. The mean number of detected pathogens was reported descriptively. In the primary resistance analysis, specimens without a reported resistance-testing result were classified as having no resistance-associated mutation. Subgroup comparisons of resistance-associated mutation rates were exploratory and were not adjusted for multiple comparisons.

Results

Participant characteristics

Among the 13,273 specimens, 7,424 (55.93%) were from boys and 5,849 (44.07%) from girls. The toddler group was the largest age group (4,555; 34.32%), followed by preschool-aged children (3,480; 26.22%), infants (2,778; 20.93%), and school-aged children (2,460; 18.53%). Most specimens were upper respiratory tract specimens (nasal or throat swabs; 12,403; 93.44%), followed by lower respiratory tract lavage specimens (823; 6.20%) and sputum specimens (47; 0.35%) (Table 2).

Table 2. Characteristics of the study specimens and comparison of tNGS positivity

Variable	Category	n	Composition, %	Positive, %	χ^2	P
Sex	Male	7424	55.93	7230 (97.39)	1.441	0.230
	Female	5849	44.07	5671 (96.96)		
Age group	Infant (28 days–1 year)	2778	20.93	2637 (94.92)	95.574	<0.001
	Toddler (1–3 years)	4555	34.32	4451 (97.72)		
	Preschool-aged (4–6 years)	3480	26.22	3428 (98.51)		
	School-aged (7–14	2460	18.53	2385 (96.95)		

Variable	Category	n	Composition, %	Positive, %	χ^2	P
	years)					
Specimen source	Upper respiratory tract group	12403	93.45	12045 (97.11)		
	Sputum group	47	0.35	43 (91.49)	12.934	0.002
	Lower respiratory lavage group	823	6.20	813 (98.78)		
Year	2023	4294	32.35	4145 (96.53)		
	2024	6061	45.66	5929 (97.82)	11.623	0.003
	2025	2918	21.98	2827 (96.88)		

Overall pathogen detection

Pathogens were detected in 12,901 of 13,273 specimens (97.20%). Positivity was 94.92% in infants, 97.72% in toddlers, 98.51% in preschool-aged children, and 96.95% in school-aged children. Positivity was 97.11% for upper respiratory tract specimens, 91.49% for sputum, and 98.78% for lower respiratory tract lavage specimens (Table 2).

Pathogen detection profile and subtype characteristics

A total of 32,525 detections of 35 pathogen categories were recorded in 13,273 specimens. The five most frequently detected pathogens were *H. influenzae* (5,400; 40.68%), rhinovirus (4,023; 30.31%), *S. pneumoniae* (3,442; 25.93%), *M. catarrhalis* (2,972; 22.39%), and *M. pneumoniae* (2,931; 22.08%). The dataset included 21 detections of *Pneumocystis jirovecii* and one detection of *Aspergillus fumigatus* (Table 3; Fig. 1).

Pathogen profiles differed by specimen type. Upper respiratory tract specimens were dominated by *H. influenzae*, rhinovirus, *S. pneumoniae*, and *M. catarrhalis*. In the lower respiratory tract lavage group (n = 823), *M. pneumoniae* was the most frequently detected pathogen (574; 69.74%), followed by *H. influenzae* (301; 36.57%), *S. pneumoniae* (232; 28.19%), rhinovirus (216; 26.25%), human adenovirus (155; 18.83%), *Staphylococcus aureus* (100; 12.15%), *M. catarrhalis* (72; 8.75%), *Chlamydia pneumoniae* (60; 7.29%), and human respiratory syncytial virus (59; 7.17%). *Pneumocystis jirovecii* (21 specimens), *Mycobacterium tuberculosis* complex (5), *Klebsiella pneumoniae* (4), *Pseudomonas aeruginosa* (1), and *Aspergillus fumigatus* (1) were also detected.

Table 3. Fifteen most frequently detected pathogens and their distribution by specimen type

Pathogen	Overall n	Detection rate, %	Upper respiratory tract group (n = 12403)	Sputum group (n = 47)	Lower respiratory lavage group (n = 823)	Category
Haemophilus influenzae	5400	40.68	5084	15	301	Bacteria
Rhinovirus	4023	30.31	3797	10	216	Virus
Streptococcus pneumoniae	3442	25.93	3187	23	232	Bacteria
Moraxella catarrhalis	2972	22.39	2886	14	72	Bacteria

Pathogen	Overall n	Detection rate, %	Upper respiratory tract group (n = 12403)	Sputum group (n = 47)	Lower respiratory lavage group (n = 823)	Category
Mycoplasma pneumoniae	2931	22.08	2353	4	574	Atypical pathogen
Human adenovirus	1989	14.99	1830	4	155	Virus
Human respiratory syncytial virus	1890	14.24	1824	7	59	Virus
Staphylococcus aureus	1815	13.67	1710	5	100	Bacteria
Human metapneumovirus	870	6.55	833	7	30	Virus
Enterovirus	862	6.49	822	2	38	Virus
Human parainfluenza virus type 3	859	6.47	825	3	31	Virus
Human bocavirus	815	6.14	777	1	37	Virus
SARS-CoV-2	698	5.26	684	1	13	Virus
Influenza virus	684	5.15	651	2	31	Virus
Bordetella pertussis	669	5.04	630	0	39	Bacteria

Note: Detection rate = number of specimens positive for the pathogen/total number of specimens (13,273) × 100%. Values by specimen type are numbers of detections within that group.

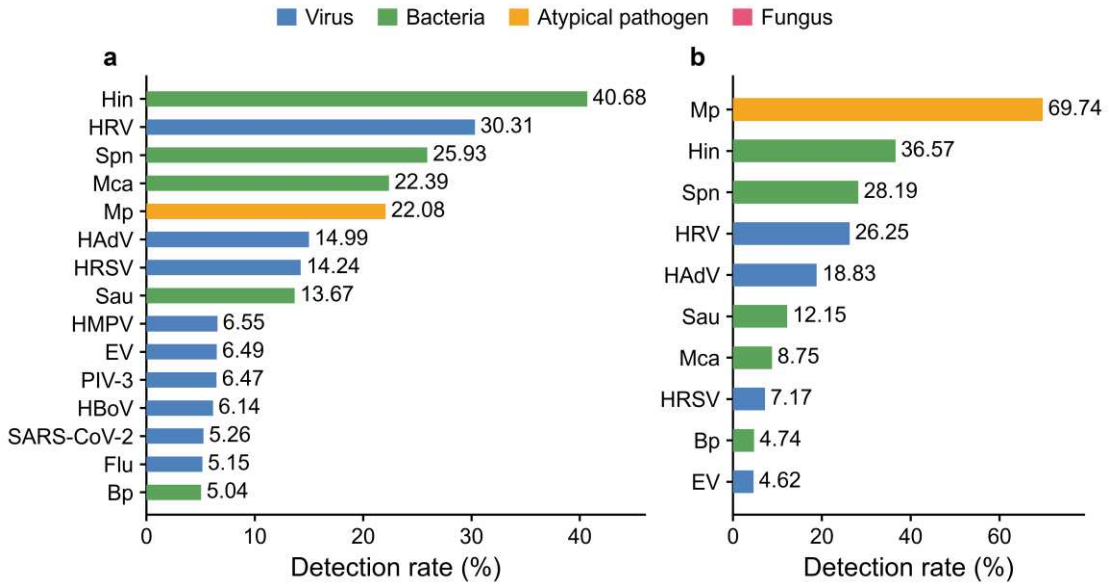


Fig. 1. Pathogen detection profiles overall and in lower respiratory tract lavage specimens. (a) Overall detection rates of the 15 most frequently detected pathogens. (b) Detection profile in the lower respiratory tract lavage group.

Pathogen detection by age group

Pathogen detection profiles differed markedly across age groups (Table 4). *H. influenzae* had the highest detection rate in every age group (28.11% in infants, 42.37% in toddlers, 48.13%

in preschool-aged children, and 41.22% in school-aged children). Rhinovirus (27.57%) and human respiratory syncytial virus (25.34%) predominated in infants; rhinovirus (33.11%) and *M. catarrhalis* (29.51%) predominated in toddlers. Detection of *S. pneumoniae* (33.76%) and *M. pneumoniae* (33.45%) increased substantially in preschool-aged children, and the highest *M. pneumoniae* detection rate was observed in school-aged children (38.66%). Detection rates of human respiratory syncytial virus and human parainfluenza virus type 3 decreased with age, whereas *M. pneumoniae* detection increased significantly with age ($\chi^2 = 1245.57$, $P < 0.001$).

Table 4. Detection of major pathogens by age group, n (%)

Pathogen	Infant (n = 2778)	Toddler (n = 4555)	Preschool-aged (n = 3480)	School-aged (n = 2460)	χ^2	P
Haemophilus influenzae	781 (28.11) ^{bcd}	1930 (42.37) ^{ac}	1675 (48.13) ^{abd}	1014 (41.22) ^{ac}	267.56	<0.001
Rhinovirus	766 (27.57) ^{bc}	1508 (33.11) ^{ad}	1099 (31.58) ^{ad}	650 (26.42) ^{bc}	46.97	<0.001
Streptococcus pneumoniae	355 (12.78) ^{bcd}	1300 (28.54) ^{acd}	1175 (33.76) ^{abd}	612 (24.88) ^{abc}	378.91	<0.001
Moraxella catarrhalis	510 (18.36) ^{bcd}	1344 (29.51) ^{acd}	838 (24.08) ^{abd}	280 (11.38) ^{abc}	335.97	<0.001
Mycoplasma pneumoniae	155 (5.58) ^{bcd}	661 (14.51) ^{acd}	1164 (33.45) ^{abd}	951 (38.66) ^{abc}	1245.57	<0.001
Human adenovirus	92 (3.31) ^{bcd}	762 (16.73) ^{ac}	749 (21.52) ^{abd}	386 (15.69) ^{ac}	425.74	<0.001
Human respiratory syncytial virus	704 (25.34) ^{bcd}	846 (18.57) ^{acd}	243 (6.98) ^{abd}	97 (3.94) ^{abc}	714.08	<0.001
Staphylococcus aureus	649 (23.36) ^{bcd}	416 (9.13) ^{ad}	379 (10.89) ^{ad}	371 (15.08) ^{abc}	327.42	<0.001
Human metapneumovirus	177 (6.37) ^{bd}	399 (8.76) ^{acd}	209 (6.01) ^{bd}	85 (3.46) ^{abc}	76.60	<0.001
Enterovirus	87 (3.13) ^{bc}	373 (8.19) ^{ad}	296 (8.51) ^{ad}	106 (4.31) ^{bc}	115.79	<0.001
Human parainfluenza virus type 3	284 (10.22) ^{cd}	401 (8.80) ^{cd}	116 (3.33) ^{ab}	58 (2.36) ^{ab}	230.92	<0.001
Human bocavirus	114 (4.10) ^{bd}	540 (11.86) ^{acd}	136 (3.91) ^{bd}	25 (1.02) ^{abc}	420.27	<0.001
SARS-CoV-2	327 (11.77) ^{bcd}	172 (3.78) ^{a}	102 (2.93) ^{a}	97 (3.94) ^{a}	302.96	<0.001
Influenza virus	104 (3.74) ^{cd}	192 (4.22) ^{cd}	235 (6.75) ^{ab}	153 (6.22) ^{ab}	43.43	<0.001
Bordetella pertussis	141 (5.08) ^{bcd}	71 (1.56) ^{acd}	266 (7.64) ^{ab}	191 (7.76) ^{ab}	202.78	<0.001

Note: Values are numbers of positive specimens, with detection rates (number positive/number of specimens in the age group, %) in parentheses. χ^2 and P values are from the overall comparison among the four groups. Superscripts a, b, c, and d indicate statistically significant pairwise differences versus infants, toddlers, preschool-aged children, and school-aged children, respectively. Pairwise analyses used Yates-corrected χ^2 tests for 2 × 2 tables and Bonferroni correction ($\alpha' = 0.05/6 \approx 0.0083$); all expected cell counts were ≥ 5, so Fisher's exact test was not used.

Temporal and seasonal distributions

After standardization by the number of specimens submitted each month, major pathogens showed clear seasonal patterns (Fig. 2). *M. pneumoniae* was detected year-round, with higher detection rates in summer (25.71%) and winter (22.95%) than in autumn (20.97%) and spring (18.27%). High-level circulation began in July 2023, with a peak monthly detection rate of 42.00% in December 2023 and a secondary peak of 41.10% in July 2024. Detection declined

sharply from the fourth quarter of 2024 (4.17% in December) and remained sporadic throughout 2025 (all months < 4%). Human respiratory syncytial virus was more frequent in winter and spring (17.87% and 20.03%, respectively), with an outbreak peak in April 2023 (53.31%). Recurring winter–spring peaks occurred thereafter (34.62% in February 2024 and 30.54% in April 2025), followed by a further increase in October 2025 (35.48%).

Influenza virus was more frequent in winter (13.03%), peaking at 24.26% in December 2025 and 22.73% in March 2023. Human parainfluenza virus type 3 peaked in summer (9.43%; 18.45% in June 2023). Human metapneumovirus was relatively frequent in autumn and winter (9.33% and 9.85%, respectively). Rhinovirus was more frequent in spring and autumn (35.62% and 40.12%, respectively), peaking at 66.07% in November 2024, whereas human adenovirus was relatively frequent in winter (21.37%). Among common bacterial pathogens, *H. influenzae* was more frequent in spring and winter (48.23% and 45.39%, respectively), *M. catarrhalis* and *S. pneumoniae* were relatively frequent in autumn (26.64% and 28.89%, respectively), and *Bordetella pertussis* was relatively frequent in spring (6.74%). Fewer specimens were submitted in January–February 2023; fluctuations at the beginning of the time series should therefore be interpreted cautiously.

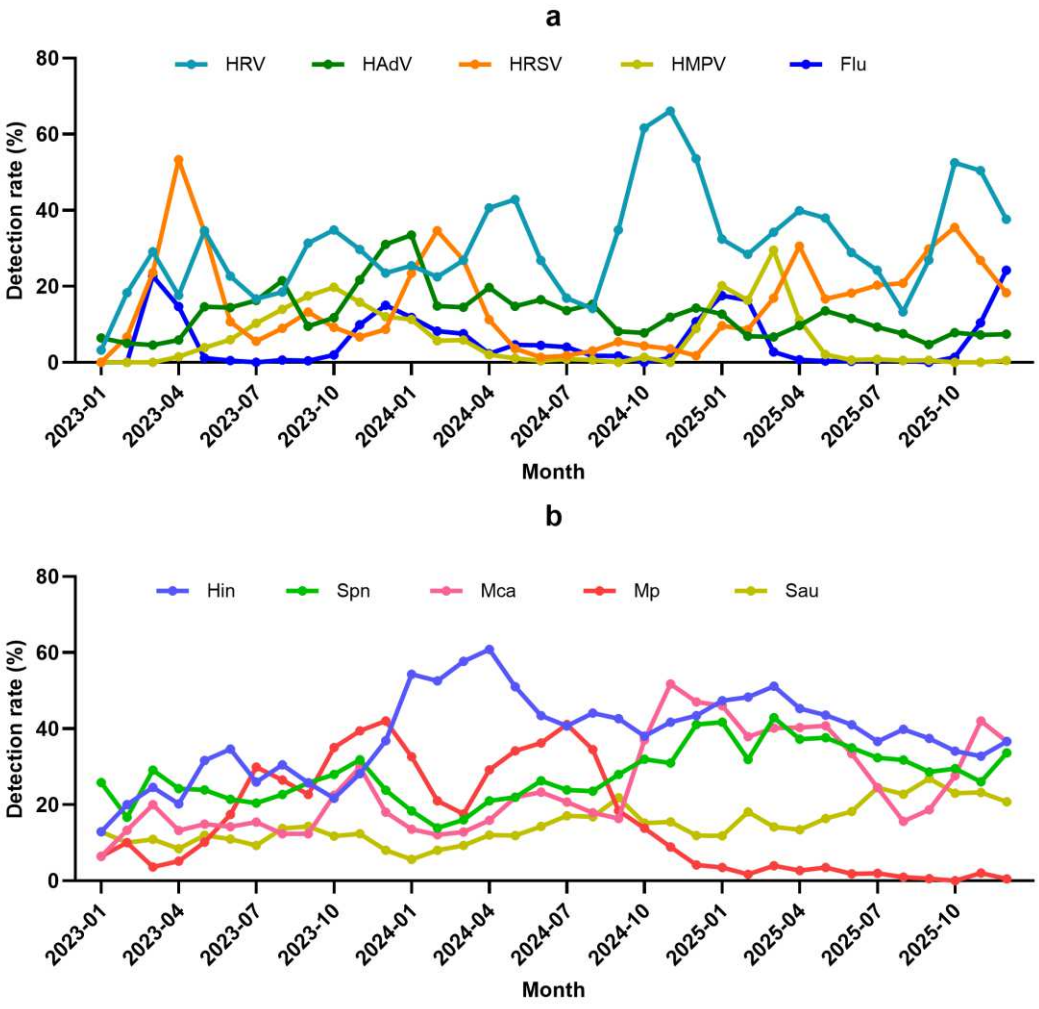


Fig. 2. Seasonal variation in monthly detection rates of major pathogens. (a) Common viruses: HRV, human rhinovirus; HRSV, human respiratory syncytial virus; HAdV, human adenovirus; HMPV, human metapneumovirus; Flu, influenza virus. (b) Common bacteria and atypical pathogens: Hin, *Haemophilus influenzae*; Spn, *Streptococcus pneumoniae*; Mca, *Moraxella catarrhalis*; Mp, *Mycoplasma pneumoniae*; Sau, *Staphylococcus aureus*.

Multiple-pathogen co-detection and dominant-pathogen analysis

Multiple-pathogen co-detection occurred in 9,983 of 12,901 positive specimens (77.38%). Single-pathogen detections occurred in 2,918 positive specimens. The distribution of detection counts is shown in Table 5. Because repeat testing was not deduplicated, these results describe testing events rather than unique children.

Multiple-pathogen co-detection rates did not differ by specimen type: 78.13% (9,433/12,073) for upper respiratory tract specimens, 76.74% (33/43) for sputum, and 77.49% (630/813) for lower respiratory tract lavage specimens ($\chi^2 = 0.229$, $P = 0.892$). However, the mean number of detected pathogens was highest in lower respiratory tract lavage specimens (2.58 vs 2.52 for upper respiratory tract specimens and 2.44 for sputum), as was the proportion with three or more detected pathogens (46.13%). Co-detection differed by age ($\chi^2 = 259.966$, $P < 0.001$), with the lowest rate in infants (68.52%), the highest rates in toddlers (82.33%) and preschool-aged children (82.90%), and a lower rate in school-aged children (73.81%).

A pathogen with a within-specimen relative abundance ≥ 50% was classified as dominant. Among specimens with multiple pathogens, 94.18% had one dominant pathogen, suggesting that most co-detection profiles comprised one dominant pathogen plus lower-abundance accompanying detections. The most common dominant pathogens were M. pneumoniae (1,405; 13.92%), H. influenzae (1,188; 11.77%), and rhinovirus (1,101; 10.91%), followed by human respiratory syncytial virus (875; 8.67%), human adenovirus (731; 7.24%), S. pneumoniae (709; 7.02%), and M. catarrhalis (692; 6.85%).

Table 5. Distribution of pathogen-category combinations by number of detected pathogens, n (%)

Pathogen-category combination	Single detection (n = 2833)	Two-pathogen detection (n = 4206)	Three-pathogen detection (n = 3256)	Four-pathogen detection (n = 1809)	Five-pathogen detection (n = 645)	≥6-pathogen detection (n = 180)
Bacteria	718(25.34)	412(9.80)	136(4.18)	18(1.00)	1(0.16)	0(0.00)
Virus	1441(50.86)	487(11.58)	85(2.61)	20(1.11)	5(0.78)	0(0.00)
Mycoplasma/*Chlamydia*	672(23.72)	7(0.17)	0(0.00)	0(0.00)	0(0.00)	0(0.00)
Bacteria + virus	/	2311(54.95)	2204(67.69)	1258(69.54)	437(67.75)	108(60.00)
Bacteria + *Mycoplasma*/*Chlamydia*	/	608(14.46)	222(6.82)	64(3.54)	14(2.17)	1(0.56)
Virus + *Mycoplasma*/*Chlamydia*	/	377(8.96)	108(3.32)	22(1.22)	5(0.78)	1(0.56)
Bacteria + virus + *Mycoplasma*/*Chlamydia*	/	/	500(15.36)	427(23.60)	183(28.37)	70(38.89)
Total	2918 (22.62)	4105 (31.82)	3210 (24.88)	1811 (14.04)	661 (5.12)	196 (1.52)

Note: Percentages for each combination are calculated within the corresponding detection-count category. Percentages in the total row are calculated among all positive specimens (n = 12,901). Mycoplasma/Chlamydia comprises M. pneumoniae, C. pneumoniae, and Chlamydia trachomatis. A slash indicates that the combination was not observed in that category. Very few specimens containing fungi were not reported separately (two single-pathogen, four two-pathogen, and one three-pathogen detections; none in the remaining categories).

Macrolide-resistance-associated mutations in *Mycoplasma pneumoniae*

Among 2,931 specimens positive for *M. pneumoniae*, 2,511 had a reported macrolide-resistance result. Of these, 2,445 were interpretable at the relevant positions and 66 were uninterpretable because sequence counts were below the analytical depth required for interpretation. A further 420 specimens (14.33%) did not have a reported macrolide-resistance item (Table 6).

Table 6. Interpretation of macrolide-resistance-associated mutations in *Mycoplasma pneumoniae*, n (%)

Stratum (year)	*M. pneumoniae*-positive specimens	No result reported	Not interpretable	Primary-analysis denominator	Predominant mutant population	Mixed population	Classified as mutation-negative	Mutation rate, %
2023	1151	298	0	1151	845(73.41)	6(0.52)	300(26.07)	73.94
2024	1720	122	57	1663	1412(84.91)	14(0.84)	237(14.25)	85.75
2025	60	0	9	51	45(88.24)	2(3.92)	4(7.84)	92.16
Total	2931	420	66	2865	2302(80.35)	22(0.77)	541(18.88)	81.12

Note: The primary-analysis denominator comprises *M. pneumoniae*-positive specimens excluding those with uninterpretable resistance results. It includes specimens without a reported resistance result, which were classified as mutation-negative. Percentages for the three interpretation categories use this denominator. The mutation rate = (predominant mutant population + mixed population)/primary-analysis denominator

× 100%.

From 2023 to 2025, macrolide-resistance-associated mutations were detected in 81.12% (2,324/2,865) of *M. pneumoniae*-positive specimens. This result used the primary analysis definition, in which specimens without a reported resistance-testing result were classified as having no resistance-associated mutation. By year, the respective rates were 73.94%, 85.75%, and 92.16%. Because the proportion of specimens without a reported resistance item differed across years, these differences should not be interpreted as evidence of a true increase in resistant strains. The mutation rate was higher in girls than boys (83.11%, 1,092/1,314 vs 79.43%, 1,232/1,551; $\chi^2 = 6.026$, P = 0.014), and varied across age groups ($\chi^2 = 9.252$, P = 0.026). No statistically significant differences were observed by specimen type or between single-pathogen and multiple-pathogen detections.

Among the 2,324 specimens with resistance-associated mutations, 23S rRNA A2063G predominated (2,310; 99.40%), followed by A2047G (36; 1.55%) and A2064G (10; 0.43%). Thirty-three specimens (1.42%) had two mutations, most commonly A2063G plus A2047G. One specimen had A2067G at a mutant allele frequency < 20%; it was interpreted as wild type and was not classified as resistant.

Macrolide-resistance-associated mutation rates differed by age group and sex but not by specimen type or detection pattern (Table 7). In the primary-analysis denominator (n = 2,865), the rate was lowest in infants (76.16%, 115/151) and highest in preschool-aged children (82.91%, 941/1,135), with intermediate values in toddlers (82.61%, 532/644) and school-aged children (78.72%, 736/935) ($\chi^2 = 9.252$, P = 0.026). Girls had a higher rate than boys (83.11%, 1,092/1,314 vs 79.43%, 1,232/1,551; $\chi^2 = 6.026$, P = 0.014). Rates did not differ significantly by specimen type (upper respiratory tract, 81.44%, 1,896/2,328; bronchoalveolar lavage fluid, 79.59%, 425/534; sputum, 100.00%, 3/3; P = 0.501) or between specimens with multiple-pathogen co-detection (80.41%, 1,757/2,185) and single-pathogen detection (83.38%, 567/680) ($\chi^2 = 2.797$, P = 0.094). Because the proportion of specimens without a reported resistance result was unbalanced across subgroups, these differences should be interpreted cautiously.

Table 7. Subgroup comparison of macrolide-resistance-associated mutation rates in *Mycoplasma pneumoniae*

Subgroup		Primary-analysis denominator	Mutation-positive, n (%)	Classified as mutation-negative, n (%)	χ^2	P
Age group	Infant (28 days–1 year)	151	115(76.16)	36(23.84)	9.252	0.026
	Toddler (1–3 years)	644	532(82.61)	112(17.39)		
	Preschool-aged (4–6 years)	1135	941(82.91)	194(17.09)		
	School-aged (7–14 years)	935	736(78.72)	199(21.28)		
Sex	Male	1551	1232(79.43)	319(20.57)	6.026	0.014
	Female	1314	1092(83.11)	222(16.89)		
Specimen type	Upper respiratory tract	2328	1896(81.44)	432(18.56)	—	0.501
	Sputum group	3	3(100.00)	0(0.00)		
	Bronchoalveolar lavage fluid	534	425(79.59)	109(20.41)		
Detection pattern	Multiple-pathogen co-detection	2185	1757(80.41)	428(19.59)	2.797	0.094
	Single detection	680	567(83.38)	113(16.62)		

Note: The macrolide-resistance-associated mutation rate was calculated as (predominant mutant population + mixed population)/primary-analysis denominator in the subgroup × 100%. Specimens without a reported resistance result were classified as having no resistance-associated mutation. Because the proportion of such specimens was unbalanced across subgroups, subgroup differences should be interpreted cautiously (overall macrolide-resistance-associated mutation rate, 81.12%; 2,324/2,865). Only three sputum specimens were included in the primary analysis, all with a mutation; these were included in the overall test but not in pairwise comparisons. As this subgroup contained cells with expected counts < 1, a χ^2 statistic was not applicable and Fisher–Freeman–Halton exact testing was used. Yates-corrected χ^2 testing was used for 2 × 2 tables. Subgroup analyses were exploratory and were not adjusted for multiple comparisons.

Discussion

We analyzed tNGS results from 13,273 respiratory specimens collected from children with respiratory infections at eight healthcare institutions in Zhuzhou. The overall pathogen positivity rate was 97.20%, close to the 96.7% positivity reported for pulmonary infection in the tNGS expert consensus (vs 36.8% with conventional methods) [9]. It was higher than rates in a multicenter Hunan study (64.1%) [13], a Shandong study (55.74%) [14], while other tNGS studies have also described high positivity and frequent mixed detections [15], and was within the 88.2%–100% range reported in recent tNGS studies [16, 17, 18]. Heterogeneity in positivity may reflect differences in study design, sampling, interpretation criteria, and season. The high positivity rate demonstrates frequent microbial detection in this tested population; it does not establish diagnostic superiority or the clinical causality of individual detections.

The five most frequently detected pathogens in Zhuzhou were *H. influenzae*, rhinovirus, *S. pneumoniae*, *M. catarrhalis*, and *M. pneumoniae*. Bacterial and viral detections were similar in frequency (45.77% vs 43.89%), consistent with post-COVID reports of reshaped respiratory pathogen profiles and a higher proportion of non-influenza viruses [6]. Rhinovirus was the most frequently detected virus, as reported in several other regions [13, 14, 16]. *M. pneumoniae* was the predominant pathogen in lower respiratory tract lavage specimens (69.74%), substantially

exceeding its detection rate in upper respiratory tract specimens. This pattern is consistent with *M. pneumoniae* as a major cause of pediatric community-acquired pneumonia and its association with lower respiratory tract involvement, consolidation, and atelectasis [19]. Detection of *P. jirovecii*, *M. tuberculosis* complex, and *A. fumigatus* in this group illustrates the range of organisms identified; their clinical significance requires case-level assessment.

H. influenzae and other common upper respiratory tract colonizers were frequently detected in every age group. Age stratification was particularly apparent for viruses and atypical pathogens: human respiratory syncytial virus was most frequent in infants (25.34%) and declined to 3.94% in school-aged children, whereas *M. pneumoniae* increased from 5.58% in infants to 38.66% in school-aged children. These patterns are consistent with previous observations [20] and indicate that age should be considered when interpreting pediatric respiratory pathogen detections and selecting empirical anti-infective therapy.

M. pneumoniae circulated intensely from July 2023 to August 2024, with monthly peaks in December 2023 (42.00%) and July 2024 (41.10%), consistent with the nationwide resurgence during 2023–2024 [21]. Detection decreased substantially from the fourth quarter of 2024 and remained sporadic in 2025. Human respiratory syncytial virus was more frequent in winter and spring, with an outbreak peak in April 2023; influenza virus and human adenovirus were more frequent in winter, human parainfluenza virus type 3 in summer, rhinovirus in spring and autumn, and *H. influenzae* in winter and spring. Although patterns varied among pathogens, they were broadly consistent with known seasonal trends and may inform regional early-warning and vaccination strategies.

Multiple-pathogen co-detection occurred in 9,983 of 12,901 positive specimens (77.38%). Single-pathogen detections occurred in 2,918 positive specimens. The distribution of detection counts is shown in Table 5. Because repeat testing was not deduplicated, these results describe testing events rather than unique children.

Dominant-pathogen analysis provides a framework for interpreting co-detection. A single pathogen with relative abundance ≥ 50% was present in 94.18% of specimens with multiple pathogens, most commonly *M. pneumoniae*, *H. influenzae*, or rhinovirus. Relative-abundance information may help clinicians interpret co-detection results, but its value for treatment decisions requires validation against clinical presentation, inflammatory markers, and patient outcomes.

Macrolide-resistance-associated mutations in *M. pneumoniae* were common in this region, with an overall rate of 81.12% (2,324/2,865) from 2023 to 2025 in the primary analysis. Because the proportion of specimens without a reported resistance item varied across years and subgroups, temporal and subgroup differences should be interpreted cautiously and do not establish a sustained increase in resistant strains. A2063G was the predominant mutation (99.40%), broadly consistent with previous reports of resistance-associated mutations in Chinese children [12]. Importantly, this study assessed the 23S rRNA genotype associated with macrolide resistance; this is not fully equivalent to in vitro antimicrobial susceptibility or clinical treatment failure.

Mechanistically, A2063G and A2064G mutations can confer high-level macrolide resistance by reducing drug-binding affinity at the 23S rRNA ribosomal target, and extensive macrolide exposure in children in China may be an important driver of resistance [22]. These findings support careful use of macrolides for pediatric *M. pneumoniae* infection, timely

reassessment of treatment in severe illness or inadequate clinical response, and consideration of tNGS-based 23S rRNA mutation detection as part of regional resistance surveillance [12].

To our knowledge, this is the first multicenter tNGS study of pediatric respiratory pathogen detections in Zhuzhou. The eight institutions included municipal general hospitals, maternal and child health institutions, and county-level hospitals, covering urban Zhuzhou and its affiliated counties and cities and establishing a regional baseline. The findings suggest that dynamic surveillance of M. pneumoniae 23S rRNA resistance-associated mutations and reassessment of empirical macrolide treatment response may be useful locally. Influenza vaccination should be completed before the influenza season, and infants should be prioritized for prevention of human respiratory syncytial virus. Because 77.38% of positive specimens had multiple-pathogen co-detection but 94.18% of these had a single dominant pathogen, interpretation should integrate relative abundance with clinical evidence rather than prompt combination or escalation of antimicrobial therapy solely because multiple pathogens are detected.

This study has several limitations. First, its retrospective design lacked complete data on clinical symptoms, disease severity, and outcomes, precluding determination of the precise pathogenic contribution of each detected organism. Dominant-pathogen analysis was based on a biological inference from read proportions and requires clinical validation. Second, the high analytical sensitivity of tNGS means that some detections may represent colonization, convalescence, or persistent nucleic acid rather than current infection; repeated adenovirus PCR positivity can, for example, reflect persistent nucleic acid [23]. Although a > 70% relative-abundance threshold was used for conditionally pathogenic organisms and background organisms and contaminants were excluded from positivity calls, interference from colonization and background sequences cannot be eliminated completely. Third, no parallel conventional diagnostic testing was included, precluding formal assessment of the incremental diagnostic value of tNGS. Similar pediatric work highlights the importance of evaluating concordance with conventional tests and clinical diagnoses [24]. The analysis was conducted at the specimen level; repeat testing of the same child could affect the independence of observations. In addition, classifying unreported resistance results as mutation-negative may underestimate mutation frequency. Finally, the data were from a single city, and public-health implications should be extrapolated in light of local epidemiology. Prospective multicenter studies with parallel conventional testing should further assess concordance between pathogen detections and clinical presentation.

Conclusions

Among 13,273 respiratory testing events recorded from 2023 to 2025, 12,901 were positive for at least one pathogen (97.20%). The dataset contained 32,525 detections of 35 pathogen categories, and 9,983 positive events had multiple-pathogen co-detection (77.38%). *M. pneumoniae* macrolide-resistance-associated mutations were identified in 2,324/2,865 events (81.12%) in the primary analysis, which classified 420 unreported resistance results as mutation-negative. A2063G predominated.

References

1. GBD 2019 Diseases and Injuries Collaborators. Global burden of 369 diseases and injuries in 204 countries and territories, 1990–2019: a systematic analysis for the Global Burden of Disease Study

2019. Lancet. 2020;396(10258):1204-22.
2. GBD 2023 Lower Respiratory Infections and Antimicrobial Resistance Collaborators. Global burden of lower respiratory infections and aetiologies, 1990-2023: a systematic analysis for the Global Burden of Disease Study 2023. Lancet Infect Dis. 2026;26(4):343-61.
3. Niu D, Gao Y, Zhang Y, et al. Systematic Review and Meta-Analysis of the Association Between Clinical Severity and Co-Infection of Human Adenovirus With Other Respiratory Pathogens in Children. J Med Virol. 2025;97(5):e70370.
4. Yi L, Tan L, Long Q, et al. Comparative diagnostic performance of metagenomic and two targeted sequencing methods in lower respiratory infection. Sci Rep. 2025;15:27365.
5. Liang A, Wu X, Zhu Y, et al. Targeted next-generation sequencing (tNGS): An upcoming application for pathogen identification in clinical diagnosis. J Infect Public Health. 2025;18(10):102936.
6. AlBahrani S, AlZahrani SJ, Al-Maqati TN, et al. Dynamic Patterns and Predominance of Respiratory Pathogens Post-COVID-19: Insights from a Two-Year Analysis. J Epidemiol Glob Health. 2024;14(2):311-8.
7. Liu P, Xu M, Lu L, et al. Resurgence of common respiratory viruses and mycoplasma pneumoniae after ending the zero-COVID policy in Shanghai. Sci Rep. 2025;15(1):1765.
8. Zhang M, Wen W, Ma Y, et al. Multicenter analysis of the *Mycoplasma pneumoniae* resurgence in China 2023–2024. Sci Rep. 2026;16:76.
9. Society of Clinical Microbiology of China International Exchange and Promotion Association for Medical and Healthcare. Expert consensus on the application and practice of targeted next-generation sequencing in infectious diseases. Zhonghua Yi Xue Za Zhi. 2024;104(48):4375-83.
10. Respiratory Group, Society of Pediatrics, Chinese Medical Association. Expert consensus on etiological diagnosis and clinical management of acute respiratory tract infection in children (2025 edition). Zhonghua Yi Xue Za Zhi. 2025;105(46):4225-38.
11. Chinese Severe Community-Acquired Pneumonia Research Collaborative Group. Guidance for interpretation of metagenomic next-generation sequencing results of bronchoalveolar lavage fluid in patients with severe community-acquired pneumonia. Int J Respir. 2023;43(1):7-14.
12. Wang YS, Zhou YL, Bai GN, et al. Expert consensus on the diagnosis and treatment of macrolide-resistant *Mycoplasma pneumoniae* pneumonia in children. World J Pediatr. 2024;20(9):901-14.
13. Long SJ, Hu R, Ouyang JP, et al. Epidemiological analysis of pediatric respiratory pathogens in Hunan, China: a retrospective multicenter study from 2022 to 2024. BMC Infect Dis. 2026;26:60.
14. Wang J, Cheng S, Zhang Y, et al. Post-pandemic surveillance of seven key respiratory pathogens using targeted next-generation sequencing (tNGS): A regional epidemiological study from Shandong, China. Diagn Microbiol Infect Dis. 2025;113(2):116931.
15. Zhang X, Tang R, Li X, et al. tNGS Reveals Predominant Mixed Viral Infections in a Multicenter Retrospective Study. Infect Drug Resist. 2025;18:5407-18.
16. Cai MY, Yi HW, Cai YQ, et al. Targeted next-generation sequencing for pathogen detection and epidemiological analysis of pediatric acute respiratory infections in Xiantao, China. Diagn Microbiol Infect Dis. 2025;113(3):117002.
17. Wang L, Yang X, Yang L, et al. Diagnostic and Clinical Value of Targeted Next-Generation Sequencing for Pediatric Respiratory Infections in Northern China. Clin Respir J. 2026;20(4):e70185.
18. Li C, Zhang X, Liu P, et al. Targeted next-generation sequencing characterization of respiratory pathogens in children with acute respiratory infection. BMC Infect Dis. 2025;25(1):675.
19. Tan J, Chen Y, Lu J, et al. Pathogen distribution and infection patterns in pediatric severe pneumonia:

A targeted next-generation sequencing study. Clin Chim Acta. 2025;565:119985.
20. Wang Q, Wu D, Zhang Y, et al. tNGS-based detection of respiratory pathogens in a single center: associations with age, gender, season, and co-infections. Front Cell Infect Microbiol. 2025;15:1663234.
21. Jiao W, Wang J, Li C, et al. Genetic factors driving the *Mycoplasma pneumoniae* outbreak among children post-COVID-19 in China: a whole genome analysis. Lancet Reg Health West Pac. 2025;59:101578.
22. Zheng L, Liu H, Xu C, et al. Macrolide-resistant *Mycoplasma pneumoniae* in children: clinical features, treatment response, and outcomes in a retrospective cohort from China. Front Pediatr. 2026;14:1812564.
23. Kalu SU, Loeffelholz M, Beck E, et al. Persistence of adenovirus nucleic acids in nasopharyngeal secretions: a diagnostic conundrum. Pediatr Infect Dis J. 2010;29(8):746-50.
24. Li L, Guo J, Chen J, et al. Targeted next-generation sequencing for pediatric lower respiratory tract infections: a retrospective study. Front Cell Infect Microbiol. 2025;15:1652949.

List of abbreviations

COVID-19: coronavirus disease 2019; HAdV: human adenovirus; HMPV: human metapneumovirus; HRSV: human respiratory syncytial virus; HRV: human rhinovirus; NCBI: National Center for Biotechnology Information; PCR: polymerase chain reaction; RI: respiratory infection; SARS-CoV-2: severe acute respiratory syndrome coronavirus 2; tNGS: targeted next-generation sequencing.

Microorganism abbreviations: *H. influenzae*, *Haemophilus influenzae*; *M. catarrhalis*, *Moraxella catarrhalis*; *M. pneumoniae*, *Mycoplasma pneumoniae*; *S. pneumoniae*, *Streptococcus pneumoniae*.

Declarations

Ethics approval and consent to participate

This study was conducted in accordance with the ethical principles of the Declaration of Helsinki (1964) and its subsequent amendments, and with the ethical standards of the institutional research committees of all participating centres. The study protocol was reviewed and approved by the Ethics Committee of Zhuzhou Central Hospital (Approval No. KY2026088-01).

Consent for publication

Not applicable.

Availability of data and materials

The datasets of this study can be obtained from the corresponding author upon reasonable request.

Competing interests

The authors declare no competing interests.

Funding

The authors declare that no financial support was received for the research and/or publication of this article.

Acknowledgements

We express our gratitude to all participants from the 8 hospitals for their assistance and

cooperation in the collection of clinical data.

Authors' information

Not applicable.

Clinical trial registration

Not applicable. This study was a retrospective, non-interventional analysis of routinely collected clinical specimens and de-identified medical records, and did not involve any prospectively registered clinical trial.

Consent to Participate declaration

The requirement for informed consent from the patients' parents or legal guardians was waived by the Ethics Committee of Zhuzhou Central Hospital because this retrospective study used previously collected and de-identified data and involved no intervention.